TITLE

Specific locations and amounts of denatured collagen and collagen-specific chaperone HSP47 in the oviducts and uteri of old cows as compared to those of heifers

[A]Raihana Nasrin Ferdousy, and [AB]Hiroya Kadokawa

[A] Faculty of Veterinary Medicine, Yamaguchi University, Yamaguchi-shi, Yamaguchi-ken 1677-1, Japan

Tel.: + 81 83 9335825; Fax: +81 83 9335938

B Corresponding author: E-mail address: hiroya@yamaguchi-u.ac.jp

Faculty of Veterinary Medicine, Yamaguchi University, Yamaguchi-shi, Yamaguchi-ken 1677-1, Japan

Tel.: + 81 83 9335825; Fax: +81 83 9335938

Running head: Denatured collagen in bovine oviducts and uteri

Abstract

Collagen, the most abundant extra-cellular matrix in oviducts and uteri, performs critical roles in pregnancies. We hypothesised that the locations and amounts of both denatured collagen and the collagen-specific molecular chaperone, 47-kDa heat shock protein (HSP47), in the oviducts and uteri of old cows are different compared to those of young heifers because of repeated pregnancies. Since detecting damaged collagen in tissues is challenging, in the first part of this study, we developed a new method that uses a denatured collagen detection reagent. Then, we compared damaged collagen in the oviducts and uteri between post-pubertal growing nulliparous heifers (22.1 ± 1.0 months old) and old multiparous cows (143.1 ± 15.6 months old). Further, we evaluated the relationship between denatured collagen and HSP47 by combining this method with fluorescence immunohistochemistry. Picro-sirius red staining showed collagen in almost all parts of the oviducts and uteri. Expectedly, damaged collagen was increased in the oviducts and uteri of old cows. However, damaged collagen and HSP47 were not located in the same area in old cows. The number of fibroblasts increased, suggesting the presence of fibrosis in the oviducts and uteri of old cows. These organs of old cows showed higher HSP47 protein amounts than those of heifers. However, the uteri, but not oviducts, of old cows showed lower HSP47 mRNA amounts than those of heifers. These findings revealed the specific location and amounts of denatured collagen and HSP47 in the oviducts and uteri of old cows compared to those of heifers.

Additional keywords: aging, fibroblast, fibrosis, infertility, ruminants, serpin family H member 1.

Introduction

Infertility increases after aging in various animals, including cows (Osoro and Wright 1992). However, little is known about the exact pathophysiological mechanisms in oviducts and uteri. Collagen, one of the most abundant extra-cellular matrix (ECM) proteins, exerts a critical role in successful pregnancies, and abnormal collagen expression is associated with recurring miscarriages in women (Li *et al.* 2019, Shi *et al.* 2020). The bovine endometrium, similar to that of other mammalians, changes morphologically throughout the oestrous cycle (Arai *et al.* 2013). Furthermore, dysregulation of ECM remodelling in bovine endometrium may impair fertility (Scolari *et al.* 2016).

Denaturation of collagen is increased due to various diseases, including cancer, osteoporosis, and arthritis (Fields 2013, Ito and Nagata 2019). Denatured collagen was studied by electron microscopy for corneal immune injury (Mohos and Wagner 1969). It was technically challenging to detect damaged collagen in tissues until the recent development of a collagen hybridising peptide (Zitnay *et al.* 2017) and a denatured collagen detection reagent (Takita *et al.* 2019). The latter is a biotin-labelled collagen-mimetic peptide that hybridises with the denatured portion of collagen. It enables the detection of denatured collagen via western blotting as well as through visualisation of heat damaged collagen fibrils in mouse fibroblasts (Takita *et al.* 2019).

Forty-seven kilodalton heat shock protein, HSP47, encoded by *SERPINH1*, is a sole procollagen-specific molecular chaperone that is essential for correct folding of the unique, triple-helical structure of collagen (Ito and Nagata 2019). HSP47 also plays important roles in the synthesis of collagen as well as in the prevention of procollagen aggregation (Duarte and Bonatto 2018). Therefore, HSP47 is central in detecting the

location of active collagen synthesis in the oviducts and uteri.

In this study, we hypothesised that the locations and amounts of both denatured collagen and HSP47 in the oviducts and uteri of old cows are different compared to those of young heifers. In the first part of this study, we developed a new method using the denatured collagen detection reagent to compare young and old oviducts and uteri. Then, we evaluated the relationship between denatured collagen and HSP47 in heifers and old cows utilising this method followed by fluorescence immunohistochemistry. Further, we compared the amounts of the mRNA and protein of HSP47 in oviducts and uteri between the old cows and heifers.

Materials and Methods

Sample collection

All experiments were performed according to the Guiding Principles for the Care and Use of Experimental Animals in the Field of Physiological Sciences (Physiological Society of Japan) and approved by the Committee on Animal Experiments of Yamaguchi University (approval no. 301).

We obtained oviductal and uterine samples from cattle managed by contract farmers in western Japan. All cattle born in Japan since 2003 are registered at birth with an individual identification number in a database of National Livestock Breeding Center of Japan. We utilised both individual identification numbers to search the database and information given by the contract farmers for the cattle in this study.

We used a previously reported method (Ferdousy *et al.* 2020) to obtain the ampulla, isthmus, caruncular (CAR), and intercaruncular (ICAR) areas as well as the uterine myometrium from healthy postpubertal, growing, young nulliparous heifers (22.1 ± 1.0 months old; Young group), and old multiparous Japanese Black beef cows (143.1 ± 15.6 months old; 9 ± 1 parities; sacrificed at least 3 months after the last parturition; Old group) at a local abattoir. The heifers and cows were at days 2 to 3, 8 to 12, 15 to 17, or 19 to 21 of the oestrous cycle (day 0 = day of oestrus), as determined via macroscopic examination of the ovaries and uterus (Miyamoto *et al.* 2000). The samples collected were from the side ipsilateral to ovulation from days 2 to 3, 8 to 12, or 15 to 17 but were from the side ipsilateral to the dominant follicle from days 19 to 21. We collected at least five samples per group per day. Half of the samples (whole tissue fragment; about 1 cm length of ampulla and isthmus; about 5 mm in width, 5 mm in length, and 2 mm in thickness of CAR, ICAR, and myometrium) were frozen in liquid nitrogen and preserved at -80°C until RNA or protein extraction was performed. The remaining half was embedded in a cryo-mould containing an optimum cutting temperature compound (Sakura Fintechnical Co. Ltd., Tokyo, Japan), and then the cryo-mould was wrapped with an aluminium foil. The cryo-moulds were then frozen in liquid nitrogen and preserved at -80°C until *in situ* detection of denatured collagen and immunohistochemistry studies were conducted.

Additionally, we measured the total collagen in tissue using picro-sirius red staining. For this purpose, we obtained the ampulla, isthmus, CAR, and ICAR from four different young nulliparous heifers (21.5 ± 0.6 months old), and four old multiparous Japanese Black beef cows (148.8 ± 12.0 months old; 9 ± 1 parities; sacrificed at least 3 months after the last parturition) at the local abattoir. The samples were stored in 4% paraformaldehyde (PFA) at 4°C for 16 h.

Development of the method for in situ detection of denatured collagen

We developed a new method for *in situ* detection of denatured collagen. As described below, this method can be combined with fluorescent immunohistochemistry.

Unfixed tissue blocks were sectioned into 15-μm-thick sections using a cryostat (CM1950, Leica Microsystems, Wetzlar, Germany) and mounted on slides (MAS coat Superfrost, Matsunami-Glass, Osaka, Japan). Next, the tissue was fixed with 4% PFA in PBS for 15 min. Some sample sections from the young group were placed on slides treated with 100 °C PBS for 2 min (pre-heated slides) or with 25 °C accutase cell detachment solution (Nacalai Tesque, Kyoto, Japan) for 30 min (digested slides) to denature collagen, whereas others were treated with ice-cold PBS (non-treated slides). We used accutase because it is a proteolytic and collagenolytic enzyme, and it is not inhibited by the possible presence of calcium and magnesium in the tissues. We tried to use also collagenase, but the structures of the tissues were broken after staining, while accutase did not significantly damage the structure. Blocking was performed by incubating the tissue sections in PBS (0.5 mL) containing 10% normal goat serum (Wako Pure Chemicals, Osaka, Japan) for 1 h at room temperature. Tissues were then treated with an avidin/biotin blocking kit (Vector Laboratories, Burlingame, CA, USA) following

126 the manufacturer's protocol. After washing twice with PBS, the slide was loaded with 5
127 μg/mL of denatured collagen detection reagent (Funakoshi, Tokyo, Japan) and incubated
128 for 60 min at room temperature in a humid box. After washing twice with PBS, the tissues
129 were incubated with streptavidin, Alexa Fluor 546 conjugate (diluted to 1 μg/mL in PBS,
130 Thermo Fisher Scientific, Waltham, MA, USA), and 1 μg/mL of 4, 6-diamino-2-
131 phenylindole (DAPI; Wako Pure Chemicals) for 60 min at room temperature. After
132 washing thrice, cover glasses were mounted using Vectashield HardSet Mounting
133 Medium (Vector Laboratories).
134 Sections were observed with a confocal microscope (LSM710; Carl Zeiss, Göttingen,
135 Germany) equipped with a 405 nm diode laser, 488 nm argon laser, 533 nm HeNe laser,
136 and 633 nm HeNe laser. Images obtained by fluorescence microscopy were scanned with
137 a 20× or 40× oil-immersion objective and recorded with a CCD camera system controlled
138 by ZEN2012 black edition software (Carl Zeiss). The exact same microscope settings
139 were used throughout immunofluorescence imaging of the ampulla, isthmus, CAR, ICAR,
140 or myometrium to compare between young and old cows. We distinguished between the
141 layers or parts of oviducts and uteri according to Banu *et al.* (2005), Hayashi *et al.* (2017),
142 and Godoy-Guzman *et al*. (2018).

143

144 *Picro-sirius red staining for total collagen*

145 The fixed tissues were dehydrated and embedded in paraffin using the Handed
146 autokinette (model 1400P, Shiraimatsu Corp. Ltd., Osaka, Japan). Thin sections (10 μm
147 thick) were cut with a sliding microtome (Yamato Kohki, Saitama, Japan) attached onto

a slide glass. The paraffin-embedded sections were de-parafinised thrice in xylene, for 5 min each, followed by de-alcohol in 100%, 100%, 90%, and 70% ethanol and ultrapure water for 5 min each. The slides were then covered in pico-sirius red staining solution (Picro-Sirius Red Stain Kit, ScyTek laboratories Inc., Logan, UT, USA) for 1 h. Following staining, the slides were washed twice with 0.5% acetic acid solution. The sections were dehydrated through three changes of 100% ethanol and cleared in three changes of xylene. After attaching the cover slip with Entellan new mounting medium (Sigma-Aldrich, St. Lous, MO, USA), the stained sections were observed under a light microscope fitted with a digital camera (Eclipse Ci, Nikon, Tokyo, Japan). The staining and light microscopy results showed collagen in red, muscle fibres and cytoplasm in yellow, and complex in orange.

RT-PCR, sequencing of amplified products, and homology search in gene databases

Total RNA (at least four per tissue) was extracted using the RNAzol RT isolation reagent (Molecular Research Centre Inc., Cincinnati, OH, USA) and treated with deoxyribonuclease. The concentration and purity of each RNA sample were evaluated by spectrophotometry (acceptable 260/280 nm ratio of absorbance, 1.8–2.1) and electrophoresis (28S:18S ratios were 2:1). Complementary DNA was synthesised using the Verso cDNA Synthesis Kit (Thermo Fisher Scientific). No reverse transcription

167 controls (NRCs) were prepared for RT-PCR; they were generated by treating the
168 extracted RNA with the same deoxyribonuclease but not with cDNA synthetase.

169 To determine the amount of *HSP47* mRNA, a primer pair was designed by Primer
170 Express v3.0 (Thermo Fisher Scientific) based on the reference sequence of bovine
171 *HSP47* [National Center for Biotechnology Information (NCBI) reference sequence of
172 bovine HSP47 is NM_001046063]. Table 1 details the primers. PCR was performed using
173 20 ng of cDNA, 20 ng RNA as the NRC or water as the no template control (NTC), and
174 polymerase (Tks Gflex DNA Polymerase, Takara Bio Inc., Shiga, Japan) under the
175 following thermocycle conditions: 94 °C for 1 min for pre-denaturation followed by 35
176 cycles of 98°C for 10 s, 60°C for 15 s, and 68°C for 30 s. PCR products were separated
177 on 1.5% agarose gel by electrophoresis with a molecular marker (Nippon Gene, Tokyo,
178 Japan), stained with Gelstar (Lonza, Allendale, NJ, USA), and observed using a charge-
179 coupled device (CCD) imaging system (GelDoc; Bio-Rad, Hercules, CA, US). The PCR
180 products were purified with the NucleoSpin Extract II kit (Takara Bio Inc.) and then
181 sequenced using one of the PCR primers and the Dye Terminator v3.1 Cycle Sequencing
182 Kit (Thermo Fisher Scientific). The sequences obtained were used as query terms with
183 which to search the homology sequence using the basic nucleotide local alignment search
184 tool (BLAST) (available on the NCBI website).
185

186 *Western blotting for HSP47 detection*

187 G*Power 3 for windows (Faul *et al.* 2007) was used to estimate the required
188 number of samples with an alpha-error probability of 0.05 and a statistical power of 0.95.
189 Five samples per day in each tissue of each group (total of 20 samples in each tissue of
190 each group) were assessed and analysed statistically. The samples were ground in liquid
191 nitrogen and homogenised using tissue protein extraction reagent (T-PER; Thermo Fisher
192 Scientific) containing Halt protease inhibitor cocktail (Thermo Scientific). The total
193 protein content of each tissue homogenate was estimated using a bicinchoninic acid kit
194 (Thermo Fisher Scientific). The extracted protein sample was boiled with Sample Buffer
195 Solution with Reducing Reagent (6x) for SDS-PAGE (09499-14; Nacalai Tesque) for 3
196 min at 100 °C. The protein samples (8,000 ng of total protein) were loaded onto a
197 polyacrylamide gel (Any KD Criterion TGX gel, Bio-Rad) along with a molecular weight
198 marker (Precision Plus Protein All Blue Standards; Bio-Rad). Then, the proteins were
199 resolved using sodium dodecyl sulphate–polyacrylamide gel electrophoresis at 100 V for
200 90 min. The proteins were transferred onto polyvinylidene fluoride (PVDF) membranes
201 (Trans-blot turbo PVDF, Bio-Rad) with electroblotting at 2.5 A and 25 V for 7 min using
202 a Trans-blot Turbo system (Bio-Rad).

203 We used a Can Get Signal Immunoreaction Enhancer kit (Toyobo Co. Ltd, Osaka,

Japan) for membrane blocking (1 h at 25 °C), primary antibody reaction (1 h at 25 °C) with an anti-HSP47 rabbit polyclonal antibody (1:400,000 dilution with immunoreaction enhancer solution; AP7366B; Abcepta Inc., San Diego, CA, USA), and secondary antibody reaction (1 h at 25 °C) with goat anti-rabbit IgG horseradish peroxidase-conjugated antibody (Bethyl Laboratories Inc., Montgomery, TX, USA; 1:400,000 dilution with immunoreaction enhancer solution). The anti-human HSP47 rabbit antibody recognizes the mature C-terminal form of human HSP47 (corresponding to amino acids 390 to 418; FLVRDTQSGSLLFIGRLVRPKGDKMRDEL). This sequence had 100% homology to amino acids 390 to 418 of the mature C-terminal form of bovine HSP47 but no homology to other bovine proteins, as determined using protein BLAST (NCBI reference sequences of human and bovine HSP47 are NP_001193943.1 and NP_001039528.1, respectively).

The protein bands were visualised using an ECL-Prime chemiluminescence kit (GE Healthcare, Amersham, UK) and a CCD imaging system (LAS-3000 Mini; Fujifilm, Tokyo, Japan). The images were exported using the Multigauge (version 3.0; Fujifilm) software. To verify the specificity of the signals, we included several negative controls in which the primary antibodies had been omitted or normal rabbit IgG (Wako Pure Chemicals) antibodies were used instead of the primary antibodies. Signal specificity was

222 also confirmed using negative controls in which the primary antibodies were pre-
223 absorbed with 5 nM antigen peptide (Scrum Inc., Tokyo, Japan).

224 The antibodies were removed from the PVDF membrane with a stripping solution
225 (Nacalai Tesque) prior to the blocking and subsequent immunoblotting with an anti-β-
226 actin mouse monoclonal antibody (1:400,000 dilution; Sigma-Aldrich).

227 All relevant bands were cropped from the exported file using Adobe Photoshop
228 element ver. 2020 (Adobe, San Jose, CA, USA) and pasted onto a graph created using
229 DeltaGraph ver. 7.5.2J (Red rock software, Salt Lake, UT, USA). ImageQuant TL
230 (version 8.2; Cytiva, Marlborough, MA, USA) software was used to measure the band
231 sizes and volumes (calculated using rolling ball background subtraction). The ~~expression~~
232 protein amount of HSP47 was normalised against β-actin.

233

234 *RT-qPCR analysis of HSP47*

235 After preparation of high-quality total RNA and cDNA synthesis using the
236 previously described protocol, *HSP47* mRNA amount was compared among the young
237 and old groups via the relative standard curve method of RT-qPCR and data analyses, as
238 described previously (Nahar and Kadokawa 2017, Ferdousy *et al.* 2020). G*Power 3 for
239 windows (Faul *et al.* 2007) was used to estimate the required number of samples with an
240 alpha-error probability of 0.05 and a statistical power of 0.95. Five cDNA samples per

day in each tissue of each group (total of 20 cDNA samples in each tissue of each group) were assessed and analysed statistically.

To prepare external standards for amplified fragments of cDNA products containing target sequences for RT-qPCR of *HSP47*(800 bp) and two housekeeping genes, *C2orf29* (562 bp) and *SUZ12* (1169 bp), PCRs were conducted as described previously (Nahar and Kadokawa 2017). The primers were designed by Primer Express Software v3.0 (Table 1). The PCR-amplified products were purified to prepare the standards, as well as to verify the DNA sequence. Then, we prepared a 6-point relative standard by 10-fold diluting the PCR products for the relative standard method.

HSP47 mRNA levels were normalised to the geometric mean of the levels of two house-keeping genes, *C2orf29* and *SUZ12*, selected using Normfinder program (Vandesompele *et al.* 2002) and amplified using previously reported primers (Rekawiecki *et al.* 2012; Nahar and Kadokawa 2017), since they are among the most stable and reliable housekeeping genes in the bovine oviducts and uterus (Walker *et al.* 2009; Nahar and Kadokawa 2017).

The mRNA level was measured in duplicate by RT-qPCR analyses with 20 ng cDNA, using CFX96 Real Time PCR System (Bio-Rad) and Power SYBR Green PCR Master Mix (Thermo Fisher Scientific), together with the 6-point relative standards, NTC, and NRC to generate the standard curve by plotting the log of the starting quantity of the dilution factor against the C_q value using appropriate software (CFXmanagerV3.1, Bio-Rad). Temperature conditions for all genes were as follows: 95°C for 10 min for pre-denaturation; five cycles each of 95°C for 15s and 66°C for 30s; and 40 cycles each of 95°C for 15s and 60°C for 60 s. Melting curve analyses were performed at 95°C for each amplicon and each annealing temperature to ensure the absence of smaller non-specific

products, such as dimers. All the C_q values of the unknown samples (22.85 ± 0.15) were between the highest (8.00) and lowest (30.33) standards for *HSP47* in RT-qPCR. Further, all the C_q values of the unknown samples were between the highest and lowest standards for *C2orf29* or *SUZ12* in RT-qPCR. Reactions with a coefficient of determination (R^2) > 0.98 and efficiency between 95 and 105% were considered optimised. The coefficients of variation of RT-qPCRs were less than 6%. The concentration of PCR products was calculated by comparing C_q values of unknown samples with the standard curve using CFXmanagerV3.1. Then, the *HSP47* amount was divided by the geometric mean of *C2orf29* and *SUZ12* in each sample.

Immunofluorescence staining and confocal microscopy

For immunofluorescence staining, we randomly selected at least five tissue samples per day in each tissue of each group. To evaluate the association between HSP47-rich areas and denatured collage-rich areas, the tissues on slides were washed once after incubation with streptavidin, Alexa Fluor 546 conjugate, and DAPI. Then, the sections were treated with 0.3% Triton X-100 for 15 min, blocked with 10% normal goat serum in PBS for 1 h at room temperature, and subjected to a primary antibody reaction with the anti-HSP47 antibody (1:1,000 dilution for overnight at 4°C). Subsequently, the samples were subjected to a secondary antibody reaction with Alexa Fluor 647 goat anti-rabbit IgG (diluted to 1 μg/mL, Thermo Fisher Scientific) and 1 μg/mL DAPI for 2 h at room temperature. After washing the sections four times, the slides were mounted in preparation for confocal microscopy. To verify the specificity of signals, we included several negative controls in which the primary antiserum had been omitted or pre-absorbed with 5 nM antigen peptide, or in which normal rabbit IgG was used instead of

289 the primary antibody. We also included negative controls in which the secondary
290 antibodies had been omitted or normal goat IgG (Wako Pure Chemicals) antibodies were
291 used instead of the secondary antibodies. Signal specificity was also confirmed using
292 negative controls in which the secondary antibodies were pre-absorbed with 5 nM normal
293 rabbit IgG.

294 Additionally, we performed immunohistochemistry to identify whether
295 cytokeratin-rich areas or vimentin-rich areas express HSP47. For this purpose, we
296 included anti-bovine pancytokeratin mouse monoclonal antibody or anti-bovine vimentin
297 mouse monoclonal antibody (both from Sigma-Aldrich, and diluted as 1:1,000) in the
298 primary antibody reaction, and Alexa Fluor 488 goat anti-mouse IgG (diluted to 1 μg/mL,
299 Thermo Fisher Scientific) in the secondary antibody reaction.

300

301 *Analysis of the 5′-flanking region of SERPINH1*

302 The 5000-nucleotide sequence of the 5′-flanking region of the SERPINH1 gene
303 (chromosome 15: 54,737,997-54,748,417) was obtained using the online Ensembl Search
304 Genome program (http://www.ensembl.org) against the bovine genome database (April.
305 2018, ARS_UCD_1.2/bosTau9). The sequence was analysed using Genetyx software v.13
306 (Genetyx, Tokyo, Japan) for the presence of consensus response element (RE) sequences
307 for oestrogen—i.e., ERE (5′-GGTCANNNTGACC-3′), ERE-like sequence (5′-
308 TGACCCCTGGGTCA-3′) (Gruber et al., 2004), and half ERE (GGTCA, TGACC, or
309 TGACT) (Liu et al., 1995), as well as for progesterone—i.e., PRE (5′-G/A G G/T AC
310 A/GTGGTGTTCT-3′) (Geserick et al., 2005) and half PRE (5′-TGTTCT-3′) (Tsai et al.,
311 1988).

312

313 *Statistical analysis*

314 The statistical analyses were performed using StatView version 5.0 for Windows
315 (SAS Institute, Inc., Cary, NC, USA). Grubb's test verified the absence of outliers. The
316 Shapiro-Wilk's test and Kolmogorov-Smirnov Lilliefors test verified the normality of
317 distribution of each variable. Two-factor analysis of variance (ANOVA) was used to
318 evaluate the effect of age (young or old), stage (days 2 to 3, 8 to 12, 15 to 17, or 19 to 21),
319 and interaction followed by post-hoc comparisons using Fisher's protected least
320 significant difference (PLSD) test for the data of RT-qPCR or western blotting for HSP47.
321 The statistical significance of differences among stages was assessed by one-factor
322 ANOVA followed by post-hoc comparisons using Fisher's PLSD test using a model
323 consisting of variance from the effect of stage and the residual. The level of significance
324 was set at $P<0.05$. Data are expressed as means ± standard errors of the mean (SEM).
325

326 **Results**

327 Picro-sirius red staining showed red or orange colour in almost all parts of the
328 ampullae, isthmuses, CAR, ICAR, and myometria (Fig. 1).

329 We successfully developed a new *in situ* assay for the detection of denatured collagen
330 (Fig. 2). The non-treated young tissues showed a very subtle signal indicating the
331 presence of denatured collagen (red). By contrast, the old samples, similar to the heated
332 and enzyme-treated young tissues, showed a strong signal indicating the presence of
333 denatured collagen in the lamina propria and muscular layer of the ampullae and
334 isthmuses. In addition, the heated young uteri showed strong signals in the luminal
335 epithelia and uterine stroma of CAR as well as in the glandular epithelia and uterine
336 stroma of ICAR, and various cells in the uterine myometria.

PCR products of a size corresponding to that of *HSP47* (470 bp) were obtained from the ampullae, isthmuses, CAR, ICAR, and myometria, as revealed by agarose gel electrophoresis (Fig. 3). Neither the NTC nor any of the NRCs yielded any PCR-amplified products. A homology search against gene databases for the sequenced amplified products revealed bovine *HSP47* (NM_001046063) as the best match, with a query coverage of 100%, an e-value of 0.0, and a maximum alignment identity of 99%. No other bovine genes displayed homology with the PCR product, indicating that the amplified product was indeed *HSP47*.

We combined the *in situ* detection method for denatured collagen with immunofluorescence staining of HSP47 in the ampulla (Fig. 4A), isthmus (Fig. 4B), CAR (Fig. 5A), ICAR (Fig. 5B), and myometrium (Fig. 5C). Robust, high-intensity fluorescence signals of denatured collagen were localised again in the above-mentioned areas of old samples but not in those of young samples. In addition, HSP47 signals were localised in the epithelial layer and superficial stroma very near to the epithelial layer of oviducts of old individuals but only weakly in those of young individuals (Fig.6). HSP47 signals were localised in the epithelia and stroma of the CAR and ICAR of old and young individuals. HSP47 signals were localised in the myometrium of old individuals but not in those of young individuals. More importantly, HSP47 rich-areas (green) and denatured collagen-rich area (red) were different because there was little colocalisation (yellow) in the merged panels. There was no signal indicating that HSP47 had colocalised with denatured collagen in the lamina propria and muscular layers of ampullae and isthmuses. Therefore, HSP47-rich and denatured collagen-rich areas were different.

Figure 7 shows the results of western blot and outcomes of two-factor ANOVA. The western blot revealed HSP47 protein in all five specimens obtained from old cows, but

only weak expression in those from young heifers (Fig. 4). Unexpectedly, an extra band at 25 kDa appeared only in old samples. The ANOVA revealed that the age effect was significant for the 47 kDa or 25 kDa bands in the ampulla, isthmus, CAR, ICAR, and myometrium, and old samples contained a higher amount of HSP47 than the young samples. The effect of stage was significant in almost all samples, except for the 47 kDa band in ampulla and isthmus, and 25 kDa band in the myometrium. The interaction between the effects of age and stage was significant only for 47 kDa and 25 kDa bands in the CAR.

Figure 8 shows the results of RT-qPCR, and outcomes of two-factor ANOVA. The age effect was significant in the CAR, ICAR, and myometrium, but not in the ampulla and isthmus. The effect of stage was significant in the ampulla, isthmus, and ICAR, but not in CAR and myometrium. The interaction between the effects of age and stage was significant only in the isthmus.

The 5′-flanking region of the bovine SERPINH1 gene was analysed for EREs, PREs, and similar sequences. Although there were no ERE, ERE-like, or PRE sequences, 19 half ERE (7 GGTCA, 7 TGACC, and 5 TGACT) and 3 half PRE sequences were identified.

Discussion

We developed a new method that uses a denatured collagen detection reagent to identify denatured collagen-rich areas. The picro-sirius red stain showed red or orange colour in almost all parts of oviduct and uterus, including the epithelium. Boos (2000) reported the presence of collagen types I, III, IV, and VI in various parts of the uterus and

384 the presence of collagen types IV and VI in the epithelium. We did not identify the
385 collagen type in this study, but collagen was present in almost all parts of the oviduct and
386 uteri. The results indicated that the levels of denatured collagen in old oviducts and uteri
387 were higher than those in the oviducts and uteri of young ones. Thus, it is possible that
388 repeated pregnancy and parturition increase the denatured collagen. Another possible
389 reason for such an increase in the levels of denatured collagen may be infection and
390 inflammation because lipopolysaccharides decrease collagen synthesis in myometrial
391 explants from women (Wendremaire *et al.* 2013).

392 The tunica mucosa of oviducts and epithelia of the endometrium are located adjacent
393 to the lumen, and thus, the structure of these layers may be susceptible to damage or
394 frequent changes. Ovarian steroid hormones drive ECM remodelling in the bovine
395 oviduct (Gonella-Diaza *et al.* 2018). Therefore, even young heifers may require collagen
396 biosynthesis because these layers provide growth factors and nutrients for embryogenesis
397 (Hugentobler *et al.* 2010; Besenfelder *et al.* 2012).

398 Little is known regarding HSP47 expression in the oviducts and uteri of all species.
399 Therefore, we were unable to compare the data obtained by the current study with those
400 of previous studies. The high HSP47 protein amounts observed in old oviducts and uteri
401 compared with those in the young oviducts and uteri was somewhat unexpected because
402 body weights of heifers were still in the phase of increasing (Inoue *et al.* 2020), and thus,
403 we speculated that increased size of the uteri and oviducts may also play a role in HSP47

expression. Little is known regarding postnatal changes associated with the sizes of bovine oviducts and uteri, as growth continues at least until 15 months of age in beef heifers (Honaramooz *et al.* 2004). However, the minimum age at first calving among about 2600 Japanese Black heifers was 21.4 months old (Inoue *et al.* 2020). Therefore, it was possible that the growth of oviducts and uteri of the young group was completed before sampling in this study.

We must be careful in interpreting the data obtained using the anti-HSP47 antibody for two reasons. First, the antibody is not recommended for immunohistochemistry in frozen sections by the supplier. However, we observed increased denatured collagen in the paraffin section in our preliminary trial using the denatured collagen detection reagent because the steps of paraffin embedding and deparaffinisation increased the denatured collagen. Second, we observed an extra 25 kDa band in the western blot. We could not find any paper reporting another size of HSP47. Therefore, we must be careful as the HSP47 signal in the immunohistochemistry results may have been caused by another protein. However, we performed western blotting using another anti-HSP47 mouse monoclonal antibody, clone M16.10A1 (Enzo Life Sciences, Inc., Farmingdale, New York. USA) and we observed both the 25 kDa and 47 kDa bands (Supplementary Figure 1). We tried to search similar proteins using the amino acid sequence of bovine HSP47 using protein BLAST. However, we could not find any protein with high homology. Therefore, further studies are required to identify the protein that the 25 kDa band corresponds to.

Importantly, HSP47 protein amount was increased in areas other than the denatured collagen-rich areas in old cows. These results suggested a possibility that collagen synthesis may not occur in denatured collagen-rich areas, indicating that a

damaged structure may remain uncured. This may explain the increased infertility observed in older beef cows (Osoro and Wright 1992).

However, this brings into question the physiological significance of increased HSP47 protein amount observed in other areas with less denatured collagen. Notably, an abnormal increase in collagen synthesis by fibroblasts induced by transforming growth factor (TGF)-β1 and its isoforms may lead to adenomyosis and ectopic endometria in women (Cheong *et al.* 2019). TGF-β1 may also exert important pathological effects on fibroblasts during equine endometriosis (Szostek-Mioduchowska *et al.* 2019). Although HSP47 is a key regulator of cell homeostasis, it also plays a role in fibrogenesis and fibrotic disorders in the liver, kidneys, and lungs. Excess HSP47 expression is an important step in collagen-related diseases, including keloids and fibrosis (Ito and Nagata, 2019). In addition, this study showed an increase in the number of fibroblasts in various parts of the oviducts and uteri, thereby suggesting fibrosis. Therefore, any increase in HSP47 protein amount may play an important role in inducing infertility in old cows.

The bovine endometrium is thicker on days 19–21 or days 2–3 than on other days (Sugiura *et al.* 2018). The highest amount of HSP47 mRNA was observed in the ampulla, isthmus, CAR, and ICAR on either days 19–21 or days 2–3 in this study. Young oviducts and uteri showed a higher amount of HSP47 mRNA than did old ones, whereas young oviducts and uteri showed a lower amount of HSP47 protein than did old ones. Based on these results, high levels of HSP47 protein may be required only temporarily in oviducts and uteri to avoid excess collagen synthesis, a possible cause for inflexibility. The HSP47 protein is bound to a ubiquitin-like protein, UBIN (Matsuda *et al.* 2001) and is degraded via the ubiquitin-proteasome system (Ito and Nagata 2016). Therefore, further studies are required to clarify the possibility that HSP47 protein is degraded via the ubiquitin-

452 proteasome system shortly after translation in young organs but is not degraded smoothly
453 in old organs, resulting in abnormal collagen synthesis.

454 HSP47 is induced by cellular stresses, but it is also constitutively expressed, and
455 its expression is always up- or down-regulated concomitantly with changes in the
456 expression of various types of collagens, as reviewed by Ito and Nagata (2017). Therefore,
457 a possible reason for the lower amount of HSP47 mRNA observed in old organs is the
458 increased collagen. We found 19 half ERE and 3 half PRE sequences in the 5'-flanking
459 region of the bovine SERPINH1 gene. A caveat here is that half ERE and PRE-like
460 sequences are only five or six nucleotides long; such short sequence can appear at random
461 at every 1024 (= 4^5) or 2048 (= 4^6) nucleotides. Thus, some of the identified sequences
462 may not be involved in the control of gene expression. Detailed studies are required to
463 clarify the mechanisms regulating HSP47 expression and the roles of oestradiol and
464 progesterone.

465 HSP47 signals were observed in the epithelial layer and superficial stroma very
466 near to the epithelial layer of oviducts and endometria of old individuals. HSP47 is
467 expressed also in the surface epithelial cells of pneumonia (Kakugawa *et al.* 2005) and
468 desmin-positive glomerular epithelium cells of the kidney (Razzaque and Taguchi 1999).
469 Moreover, HSP47 expression in human nasal mucosa and lacrimal sac (obtained
470 surgically) is associated with surgical outcome (Park *et al.* 2018). HSP47 induces
471 mesenchymal phenotypes in mammary epithelial cells for cancer metastasis, and HSP47
472 is a hub of the ECM transcription network (Xiong *et al.* 2020). Therefore, further studies
473 are required to clarify the relationship between HSP47expression in the layers and fertility
474 in cows.

475 Takita *et al.* (2019) produced a standard curve based on an enzyme immunoassay

(EIA) utilising the denatured collagen detection reagent and heated pure collagen (grade for culture dish coating). However, our attempts of immunoassays (HRP-conjugated streptavidin for EIA, fluorochrome-conjugated streptavidin for fluorescent immunoassay, lanthanide-conjugated streptavidin for dissociation-enhanced lanthanide fluorescence immunoassay) failed to obtain a good parallel between the standard curve and serially diluted bovine oviduct or uterine extracts that were extracted using various methods. This was due to the samples showing strong matrix effects unlike pure collagen. Therefore, our comparison could be performed only on photographic images.

In conclusion, these findings revealed the specific location and amounts of damaged collagen and HSP47 in the oviducts and uteri of old cows compared to those in heifers.

Acknowledgments

Raihana Nasrin Ferdousy was supported by a scholarship from MEXT (Ministry of Education, Culture, Sports, Science, and Technology). This research was partly supported by a Grant-in Aid for Scientific Research (JSPS Kakenhi Grant Number 21H02345) from Japan Society for the Promotion of Science (Tokyo, Japan) to Hiroya Kadokawa. The authors thank Prof. Ken Takeshi Kusakabe from the Laboratory of Veterinary Anatomy, Yamaguhi University, Japan, for the advice regarding picro-sirius red staining.

Conflicts of Interest

The authors declare no conflicts of interest.

References

Arai, M., Yoshioka, S., Tasaki, Y., and Kiyoshi Okuda, K. (2013). Remodeling of bovine endometrium throughout the estrous cycle. *Anim. Reprod. Sci.* **142**, 1-9. doi: 10.1016/j.anireprosci.2013.08.003

Banu, S.K., Arosh, J.A., Chapdelaine, P., and Fortier, M.A. (2005). Expression of prostaglandin transporter in the bovine uterus and fetal membranes during pregnancy. *Biol. Reprod.* **73**, 230-6. doi: 10.1095/biolreprod.105.039925

Besenfelder, U., Havlicek, V., and Brem, G. (2012). Role of the oviduct in early embryo development. *Reprod. Domest. Anim.* **47**, 156-63. doi:10. 1111/J.1439-0531.2012.02070.X 50

Boos, A. (2000). Immunohistochemical assessment of collagen types I, III, IV and VI in biopsy samples of the bovine uterine wall collected during the oestrous cycle. *Cells Tissues Organs* **167**, 225-38. doi: 10.1159/000016799.

Cheong, M.L., Lai, T.H., and Wu, W.B. (2019). Connective tissue growth factor mediates transforming growth factor β-induced collagen expression in human endometrial stromal cells. *PLoS One* **14**, e0210765. doi: 10.1371/journal.pone.0210765

Duarte, B.D.P., and Bonatto, D. (2018). The heat shock protein 47 as a potential biomarker and a therapeutic agent in cancer research. *J. Cancer. Res. Clin. Oncol.* **144**, 2319-28. doi: 10.1007/s00432-018-2739-9

Faul, F., Erdfelder, E., Lang, A.G., and Buchner, A. (2007). G*Power 3: a flexible statistical power analysis program for the social, behavioral, and biomedical sciences. *Behav. Res. Methods* **39**, 175-91. doi: 10.3758/bf03193146

Ferdousy, R.N., Kereilwe, O., and Kadokawa, H. (2020). Anti-Müllerian hormone

receptor type 2 (AMHR2) expression in bovine oviducts and endometria: comparison of AMHR2 mRNA and protein abundance between old Holstein and young and old Wagyu females. *Reprod. Fertil. Dev.* **32**, 738-47. doi: 10.1071/RD19121

Fields, G.B. (2013). Interstitial collagen catabolism. *J. Biol. Chem.* **288**, 8785-93. doi: 10.1074/jbc.R113.451211

Geserick, C., Meyer, H.A., and Haendler, B. (2005). The role of DNA response elements as allosteric modulators of steroid receptor function. *Mol. Cell. Endocrinol.* **236**, 1-7. doi: 10.1016/j.mce.2005.03.007

Godoy-Guzmán, C., Nuñez, C., Orihuela, P., Campos, A., and Carriel, V. (2018). Distribution of extracellular matrix molecules in human uterine tubes during the menstrual cycle: a histological and immunohistochemical analysis. *J. Anat.* **233**, 73-85. doi: 10.1111/joa.12814

Gonella-Diaza, A. M., Mesquita, F. S., Lopes, E., Silva, K. R. d., Cogliati, B., Strefezzi R. D. F., and Binelli, M. (2018). Research Article Sex steroids drive the remodeling of oviductal extracellular matrix in cattle. *Biol. Reprod.* **99**, 590-9. doi:10.1093/biolre/ioy083

Gruber, C.J., Gruber, D.M., Gruber, I.M., Wieser, F., and Huber J.C. (2004). Anatomy of the estrogen response element. *Trends Endocrinol. Metab.* **15**, 73-8. doi: 10.1016/j.tem.2004.01.008

Hayashi, K.G., Hosoe, M., Kizaki, K., Fujii, S., Kanahara, H., Takahashi, T., and Sakumoto, R. (2017). Differential gene expression profiling of endometrium during the mid-luteal phase of the estrous cycle between a repeat breeder (RB)

545 and non-RB cows. *Reprod. Biol. Endocrinol.* **15**, 20. doi: 10.1186/s12958-017-
546 0237-6
547 Honaramooz, A., Aravindakshan, J., Chandolia, R.K., Beard, A.P., Bartlewski, P.M.,
548 Pierson, R.A., and Rawlings, N.C. (2004) Ultrasonographic evaluation of the
549 pre-pubertal development of the reproductive tract in beef heifers. *Anim. Reprod.*
550 *Sci.* **80**, 15-29. doi: 10.1016/S0378-4320(03)00136-2
551 Hugentobler, S. A., Sreenan, J. M., Humpherson, P. G., Leese, H. J., Diskin, M. G., and
552 Morris, D. G. (2010). Effects of changes in the concentration of systemic
553 progesterone on ions, amino acids and energy substrates in cattle oviduct and
554 uterine fluid and blood. *Reprod. Fertil. Dev.* **22**, 684-94. doi:10.1071/RD09129
555 Inoue, K., Hosono, M., Oyama, H., and Hirooka, H. (2020). Genetic associations between
556 reproductive traits for first calving and growth curve characteristics of Japanese
557 Black cattle. *Anim. Sci. J.* **91**, e13467. doi: 10.1111/asj.13467
558 Ito, S., and Nagata, K. (2016). Mutants of collagen-specific molecular chaperone Hsp47
559 causing osteogenesis imperfecta are structurally unstable with weak binding
560 affinity to collagen. *Biochem. Biophys. Res. Commun.* **469**, 437-42. doi:
561 10.1016/j.bbrc.2015.12.028
562 Ito, S., and Nagata, K. (2017). Biology of Hsp47 (Serpin H1), a collagen-specific
563 molecular chaperone. *Semin. Cell. Dev. Biol.* **62**, 142-51. doi:
564 10.1016/j.semcdb.2016.11.005
565 Ito, S., and Nagata, K. (2019). Roles of the endoplasmic reticulum-resident, collagen-
566 specific molecular chaperone Hsp47 in vertebrate cells and human disease. *J.*
567 *Biol. Chem.* **294**, 2133-41. doi: 10.1074/jbc.TM118.002812

568 Kakugawa, T., Mukae, H., Hayashi, T., Ishii, H., Nakayama, S., Sakamoto, N., Yoshioka,
569 S., Sugiyama, K., Mine, M., Mizuta, Y., and Kohno, S. (2005). Expression of
570 HSP47 in usual interstitial pneumonia and nonspecific interstitial pneumonia.
571 *Respir. Res.* 6, 57. doi: 10.1186/1465-9921-6-57
572 Li, M., Yao, L., Xin M., and Gao, M. (2019). Dysregulation of collagen expression in
573 peri-implantation endometrium of women with high ovarian response. *J. Obstet.*
574 *Gynaecol. Res.* **45**, 1035-44. doi: 10.1111/jog.13936
575 Liu, D., Xiong, F., and Hew, C.L. (1995). Functional analysis of estrogen-responsive
576 elements in chinook salmon (Oncorhynchus tschawytscha) gonadotropin II beta
577 subunit gene. *Endocrinology* **136**, 3486-93. Doi: 10.1210/endo.136.8.7628385
578 Matsuda, M., Koide, T., Yorihuzi, T., Hosokawa, N., and Nagata K. (2001). Molecular
579 cloning of a novel ubiquitin-like protein, UBIN, that binds to ER targeting signal
580 sequence. *Biochem. Biophys. Res. Commun*. **280**, 535-40. doi:
581 10.1006/bbrc.2000.4149
582 Miyamoto, Y., Skarzynski, D. J., and Okuda, K. (2000). Is tumor necrosis factor alpha a
583 trigger for the initiation of endometrial prostaglandin F(2alpha) release at
584 luteolysis in cattle? *Biol. Reprod*. **62**, 1109-15. doi: 10.1095/biolreprod62.5
585 Mohos, S.C., and Wagner, B.M. (1969). Damage to collagen in corneal immune injury.
586 Observation of connective tissue structure. *Arch. Pathol.* **88**, 3-20. PMID:
587 4893570
588 Nahar, A., and Kadokawa, H. (2017). Expression of macrophage migration inhibitory
589 factor (MIF) in bovine oviducts is higher in the postovulatory phase than during
590 the oestrus and luteal phase. *Reprod. Fertil. Dev.* **29**, 1521-9. doi:
591 10.1071/RD15546

592 Osoro, K., and Wright, I. A. (1992). The effect of body condition, live weight, breed, age,
593 calf performance, and calving date on reproductive performance of spring-
594 calving beef cows. *J. Anim. Sci*. **70**, 1661-6. doi: 10.2527/1992.7061661x
595 Park, J., Lee, J., and Baek, S. (2018). Pathologic features and expression of heat shock
596 protein 47 in the nasal mucosa and lacrimal sac: does it influence the surgical
597 outcome of endoscopic endonasal dacryocystorhinostomy? *Eye (Lond).* 32,
598 1432-9. doi: 10.1038/s41433-018-0115-2
599 Ray, I.L., Dumas, M., Sagot, P., and Bardou, M., (2013). Effects of leptin on
600 lipopolysaccharide-induced remodeling in an in vitro model of human
601 myometrial inflammation. *Biol. Reprod.* **88,** 45. doi:
602 10.1095/biolreprod.112.104844
603 Razzaque, M.S., and Taguchi, T. (1999). Role of glomerular epithelial cell-derived heat
604 shock protein 47 in experimental lipid nephropathy. *Kidney Int. Suppl.* **71,** S256-
605 9. doi: 10.1046/j.1523-1755.1999.07169.x
606 Rekawiecki, R., Rutkowska, J., and Kotwica, J. (2012). Identification of optimal
607 housekeeping genes for examination of gene expression in bovine corpus luteum.
608 *Reprod. Biol.* **12**, 362-7. doi: 10.1016/j.repbio.2012.10.010
609 Scolari, S.C., Pugliesi, G., Strefezzi, R.F., Andrade, S.C., Coutinho, L.L., and Binelli, M.
610 (2016). Dynamic remodeling of endometrial extracellular matrix regulates
611 embryo receptivity in cattle. *Reproduction* REP-16-0237. doi: 10.1530/REP-16-
612 0237
613 Shi, J.W., Lai Z.Z., Yang, H.L., Yang, S.L., Wang, C.J., Ao, D., Ruan, L.Y., Shen, H.H.,
614 Zhou, W.J., Mei, J., Fu, Q., and Li, M.Q. (2020). Collagen at the maternal-fetal

615 interface in human pregnancy. *Int. J. Biol. Sci.* **16**, 2220-34. doi:
616 10.7150/ijbs.45586
617 Sugiura, T., Akiyoshi, S., Inoue, F., Yanagawa, Y., Moriyoshi, M., Tajima, M., and
618 Katagiri S. (2018). Relationship between bovine endometrial thickness and
619 plasma progesterone and estradiol concentrations in natural and induced estrus.
620 *J. Reprod. Dev.* **64**, 135-43. doi: 10.1262/jrd.2017-139.
621 Szóstek-Mioduchowska, A., Słowińska, M., Pacewicz, J., Skarzynski., D.J., and Okuda,
622 K. (2020). Matrix metallopeptidase expression and modulation by transforming
623 growth factor-β1 in equine endometrosis. *Sci. Rep.* **10**, 1119. doi:
624 10.1038/s41598-020-58109-0
625 Takita, K.K., Fujii, K.K., Ishii, K., and Koide, T. (2019). Structural optimization of cyclic
626 peptides that efficiently detect denatured collagen. *Org. Biomol. Chem.* **17**, 7380-
627 7. doi: 10.1039/c9ob01042d
628 Tsai, S.Y., Carlstedt-Duke, J., Weigel, N.L., Dahlman, K., Gustafsson, J.A., Tsai, M.J.,
629 and O'Malley, B.W. (1988). Molecular interactions of steroid hormone receptor
630 with its enhancer element: evidence for receptor dimer formation. *Cell* **55**, 361-
631 9. doi: 10.1016/0092-8674(88)90059-1
632 Vandesompele, J., De Preter, K., Pattyn, F., Poppe, B., Van Roy, N., De Paepe, A., and
633 Speleman, F. (2002). Accurate normalisation of real-time quantitative RT-PCR
634 data by geometric averaging of multiple internal control genes. *Genome Biol.* **3**,
635 research0034.1–research0034.11. doi:10.1186/gb-2002-3-7-research0034
636 Walker, C.G., Meier, S., Mitchell, M.D., Roche, J.R., and Littlejohn, M. (2009).
637 Evaluation of real-time PCR endogenous control genes for analysis of gene
638 expression in bovine endometrium. *BMC Mol. Biol.* **10**, 100. doi: 10.1186/1471-

2199-10-100

Wendremaire, M., Mourtialon, P., Goirand, F., Lirussi, F., Barrichon, M., Hadi, T., Garrido, C., Ray, I.L., Dumas, M., Sagot, P., and Bardou, M. (2013). Effects of leptin on lipopolysaccharide-induced remodeling in an in vitro model of human myometrial inflammation. *Biol. Reprod.* **88,** 45. doi: 10.1095/biolreprod.112.104844

Xiong, G., Chen, J., Zhang, G., Wang, S., Kawasaki, K., Zhu, J., Zhang, Y., Nagata, K., Li, Z., Zhou, B.P., and Xu, R. (2020). Hsp47 promotes cancer metastasis by enhancing collagen-dependent cancer cell-platelet interaction. *Proc. Natl. Acad. Sci. U. S. A.* 117, 3748-58. doi: 10.1073/pnas.1911951117

Zitnay, J.L., Li, Y., Qin, Z., San, B.H., Depalle, B., Reese, S.P., Buehler, M.J., Yu, S.M., and Weiss, J.A. (2017). Molecular level detection and localization of mechanical damage in collagen enabled by collagen hybridizing peptides. *Nat. Commun.* **8**, 14913. doi: 10.1038/ncomms14913

654 **Table 1.** Details of the primers used for PCRs.

Gene	Primer	Sequence 5′-3′	Position		Size (bp)
			Nucleotide	Exon	
HSP47	Forward	GACAACCGAGGCTTCATGGT	770	4	470
	Reverse	AGCTCCTCACGCCCGTAGAT	1239	6	
C2orf29	Forward	AAGTTTTTTCTTTCCCAGCTCATG	666–688	2	562
	Reverse	CAGGAAGTTTGGCTGGAGTGA	1207–1227	5	
SUZ12	Forward	GGAAGAGACTGCCTCCATTTGA	1019–1040	10	1169
	Reverse	CCCTGAGACACCATCTGTTTCC	2166–2187	16	
HSP47	Forward	TGTCGGGCAAGAAGGACCTA	1131	5	800
	Reverse	AAAATGGGGAGGAAAGTGGG	1930	6	
HSP47	Forward	ACAAGATGCGAGACGAGTTGT	1347	5	93
	Reverse	CCCTGTTTTCCCACCCATGT	1439	5&6	
C2orf29	Forward	TCAGTGGACCAAAGCCACCTA	928–948	3	170
	Reverse	CTCCACACCGGTGCTGTTCT	1077–1097	4	
SUZ12	Forward	CATCCAAAAGGTGCTAGGATAGATG	1441–1465	13	160
	Reverse	TTGGCCTGCACACAAGAATG	1581–1600	14	

655

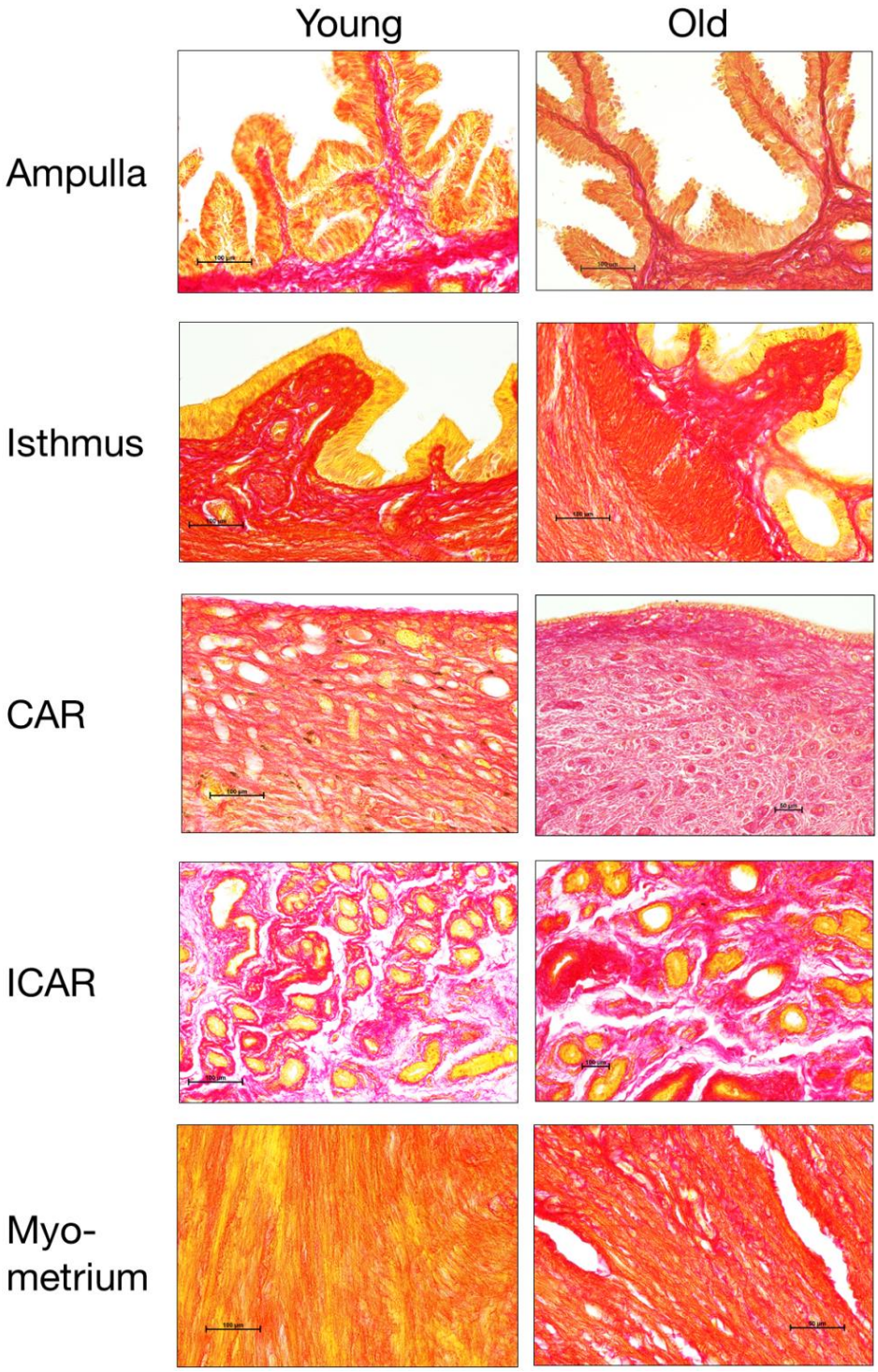

Fig. 1. Picro-sirius red staining for total collagen in ampulla, isthmus, and caruncular (CAR) and intercaruncular (ICAR) areas of the endometrium and myometrium in healthy postpubertal, growing and young nulliparous heifers (Young), and old multiparous Japanese Black beef cows (Old). The Picro-sirius red staining shows collagen in red, muscle fibres and cytoplasm in yellow, and complex in orange.

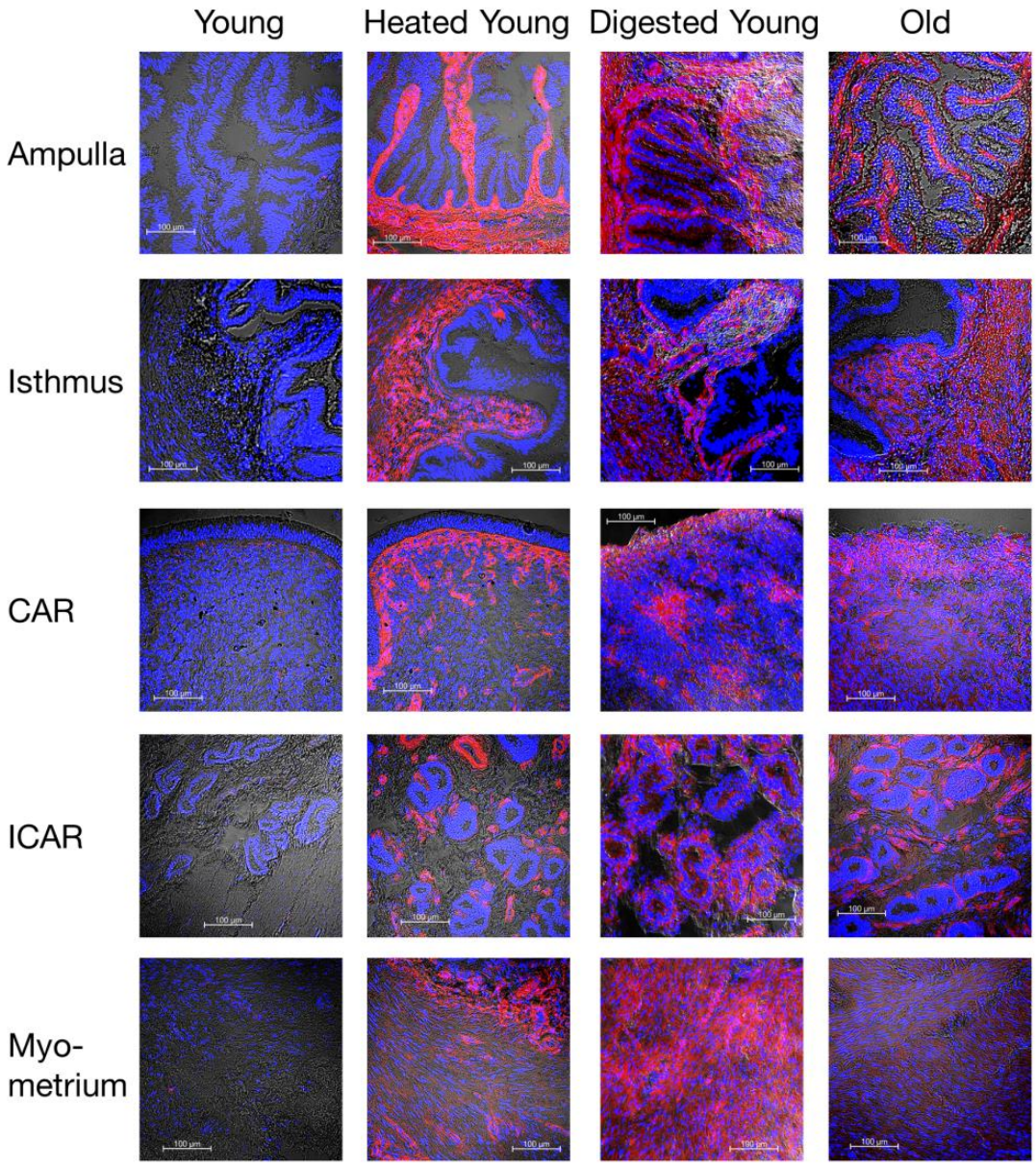

Fig. 2. *In situ* detection of denatured collagen. The no-heated, non-digested young tissues show very subtle signals of denatured collagen (red). In contrast, the old samples, in a manner similar to the heated or enzyme-digested young tissues, show strong signals corresponding to denatured collagen in the lamina propria and muscular layers of ampullae and isthmuses; the stroma of CAR and ICAR; the glandular epithelium of ICAR; and various myometrial cells.

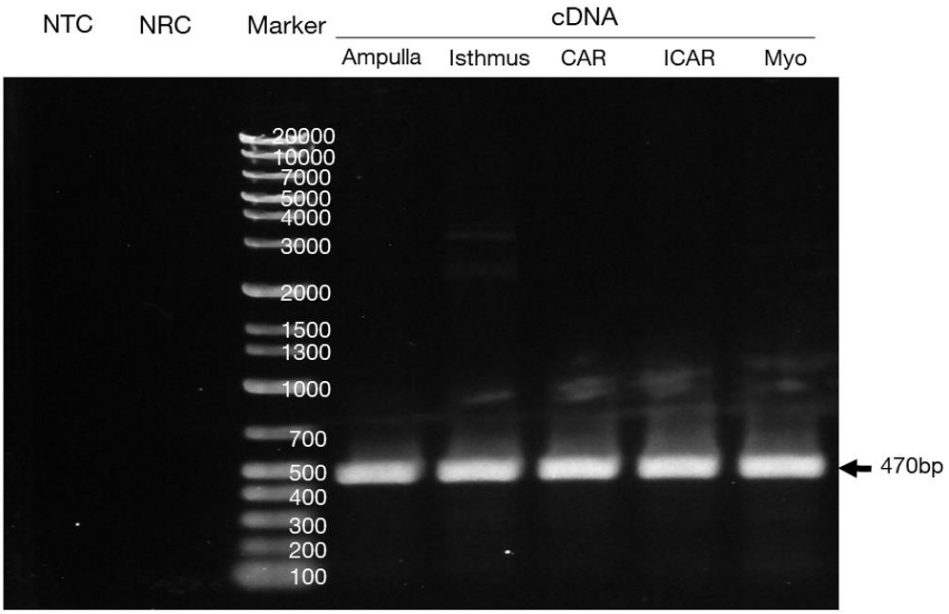

669

670

671 **Fig. 3.** Expression of heat shock protein (HSP47) detected via RT-PCR analysis. The
672 electropherogram shows the size (470 bp) expected from PCR products of bovine *HSP47*
673 in the ampulla, isthmus, CAR, ICAR, and myometrium (Myo) in old cows. Bands were
674 not present in the no template control (NTC) and no reverse transcription control (NRCs)
675 lanes.

676

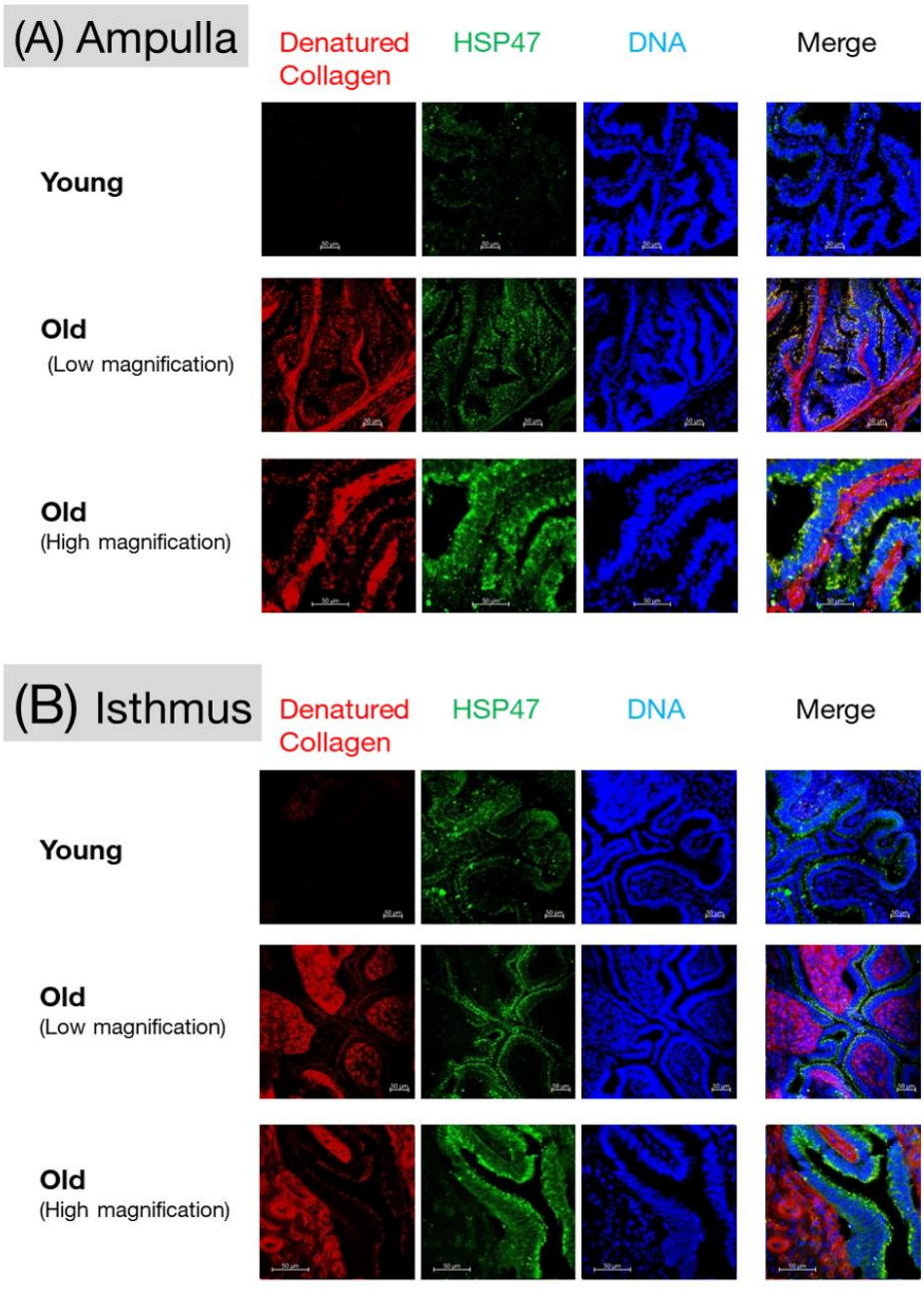

Fig. 4. Comparison of denatured collagen-rich areas (red) and HSP47-rich areas (green) in the ampullae or isthmuses (collected on day 3 of the oestrous cycle) of Young and Old groups. Nuclei are counterstained with DAPI (dark blue). Unlike the Young, the Old specimens showed strong signal corresponding to denatured collagen in the lamina propria and muscular layers. The Old specimens showed strong signal corresponding to HSP47 in the epithelia of tunica mucosa and superficial stroma. Not many signals corresponding to colocalisation (yellow) were present in the Merge panels; scale bars are 50 μm.

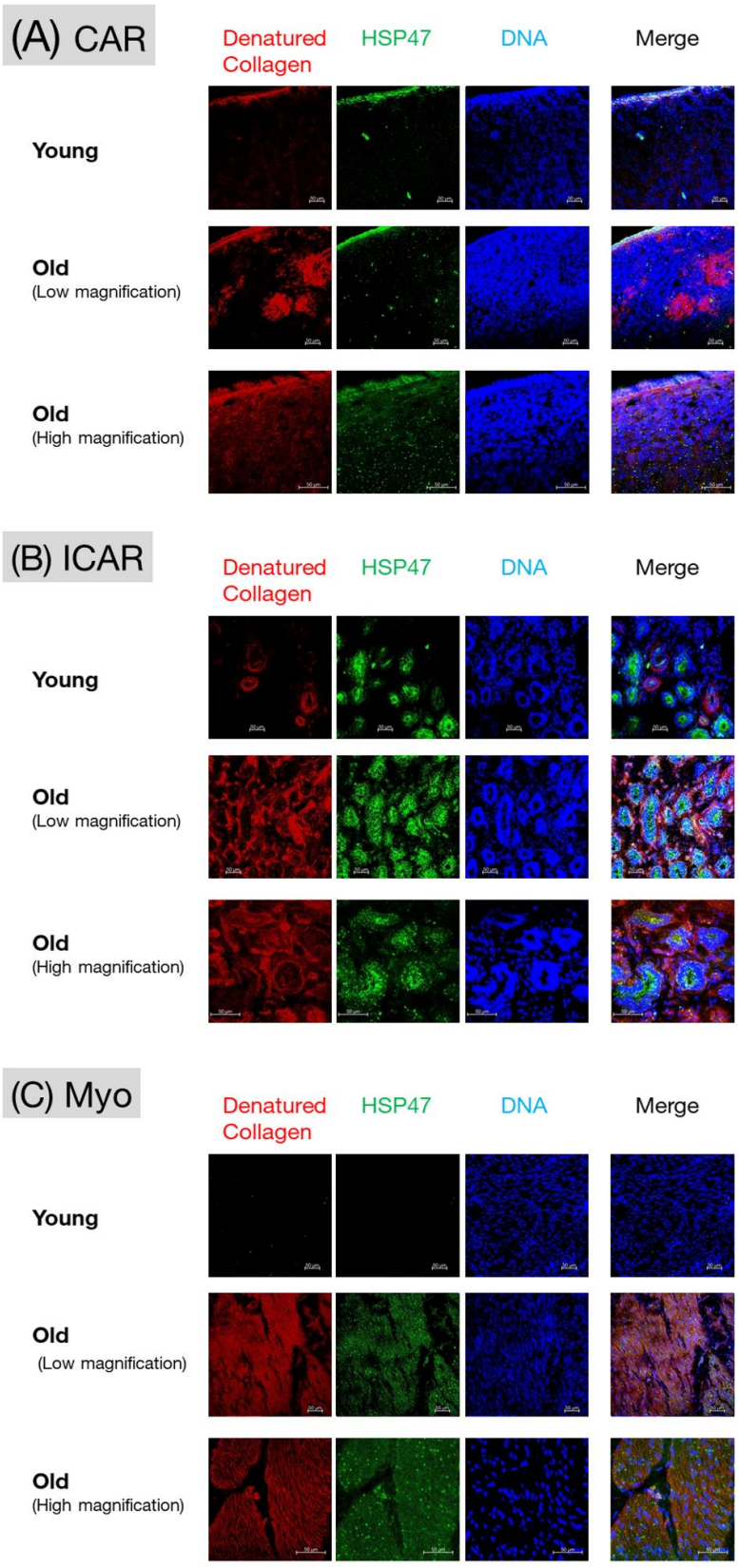

686

687 **Fig. 5.** Comparison of denatured collagen-rich areas (red) and HSP47-rich areas (green)

in the CAR, ICAR, or Myo (collected on day 13 of the oestrous cycle) of Young and Old groups. Nuclei are counterstained with DAPI (dark blue). Both the Young and Old specimens showed signals corresponding to both denatured collagen and HSP47 in luminal epithelia, glandular epithelia, and stroma. Unlike the Young, the Old specimens also showed strong signals corresponding to both denatured collagen and HSP47 in the stroma and myometria. Particularly, the number of fibroblasts (green dots) increased. However, not many signals corresponding to colocalisation (yellow) were present in the Merge panels; scale bars are 50 μm. The dark patches in old myometria are broken parts.

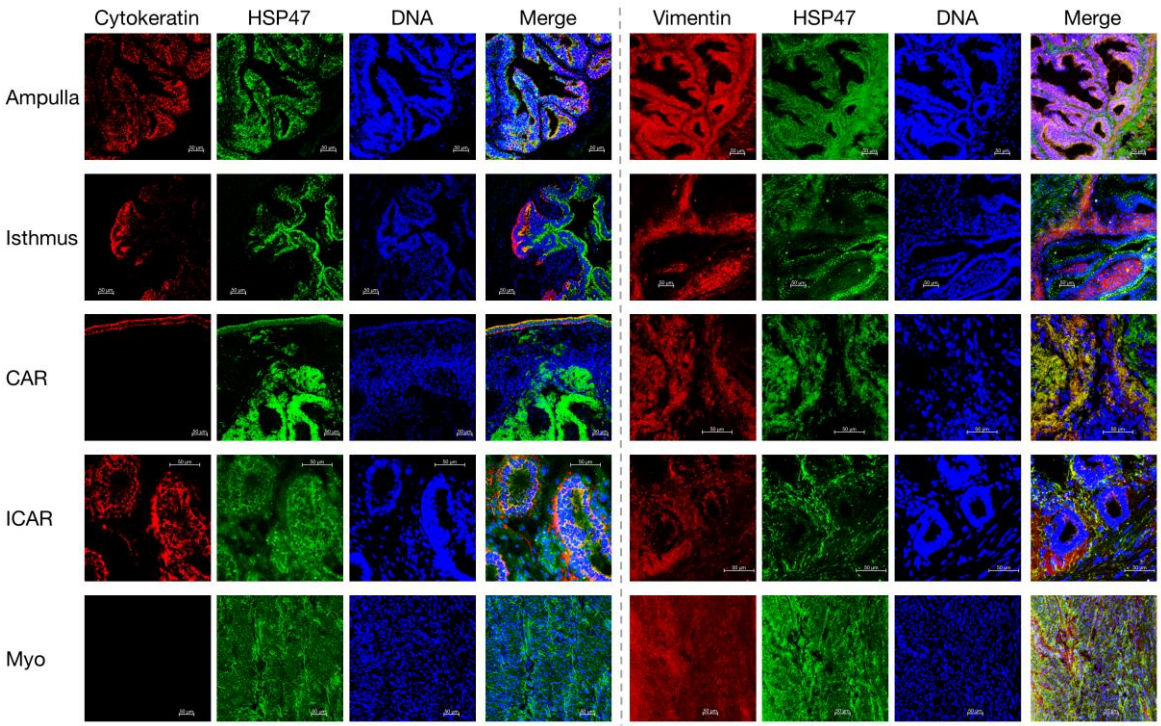

Fig. 6. Comparison of HSP47-rich areas (green) and cytokeratin- or vimentin-rich areas (red) in the ampullae or isthmuses (collected on day 3 of the oestrous cycle), or the CAR, ICAR, or Myo (collected on day 13 of the oestrous cycle) of Old groups. Nuclei are counterstained with DAPI (dark blue); scale bars are 50 μm.

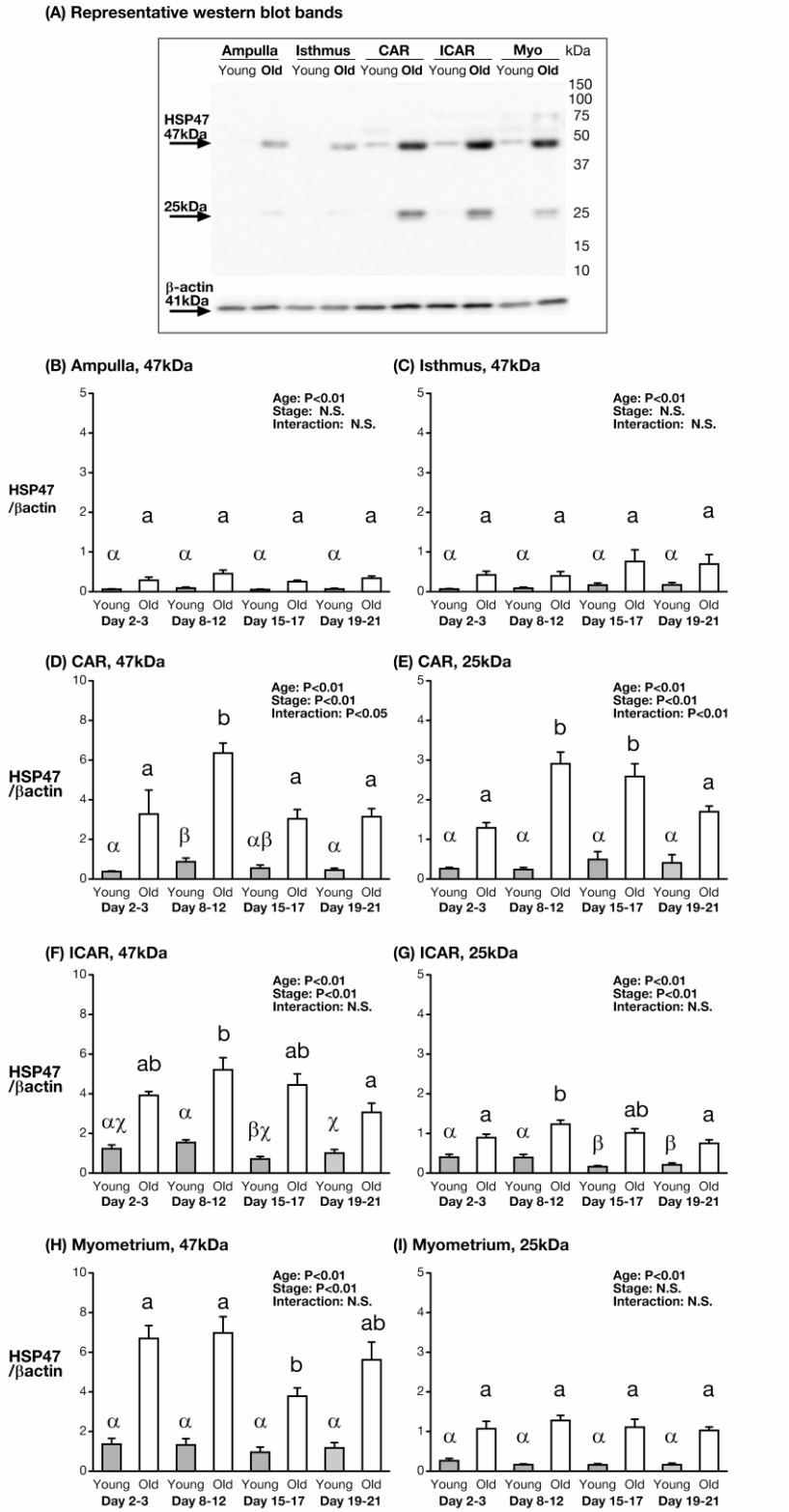

Fig. 7. Representative photos of western blotting analysis for HSP47 or anti-β−actin mouse antibodies in extracts from ampulla, isthmus, CAR, ICAR, and myometrium (Myo) in the Young and Old groups (A). Relative HSP47 protein levels normalised to

those of β-actin in the ampulla (B), isthmus (C), CAR (D), ICAR (E), or myometrium (F) in the Young and Old groups. The header in the upper corner of each graph represents the results of two-factor ANOVA followed by Fisher's PLSD test, including the effect of age (Young or Old) and effect of stage and interaction. Greek letters (α, β, or χ) above the grey left-side bars indicate significant between-stage differences in expression in Young samples; letters (a, b, or c) above the white right-side bars indicate significant between-stage differences in expression in Old samples (one-factor ANOVA followed by Fisher's PLSD test).

N.S., non-significant.

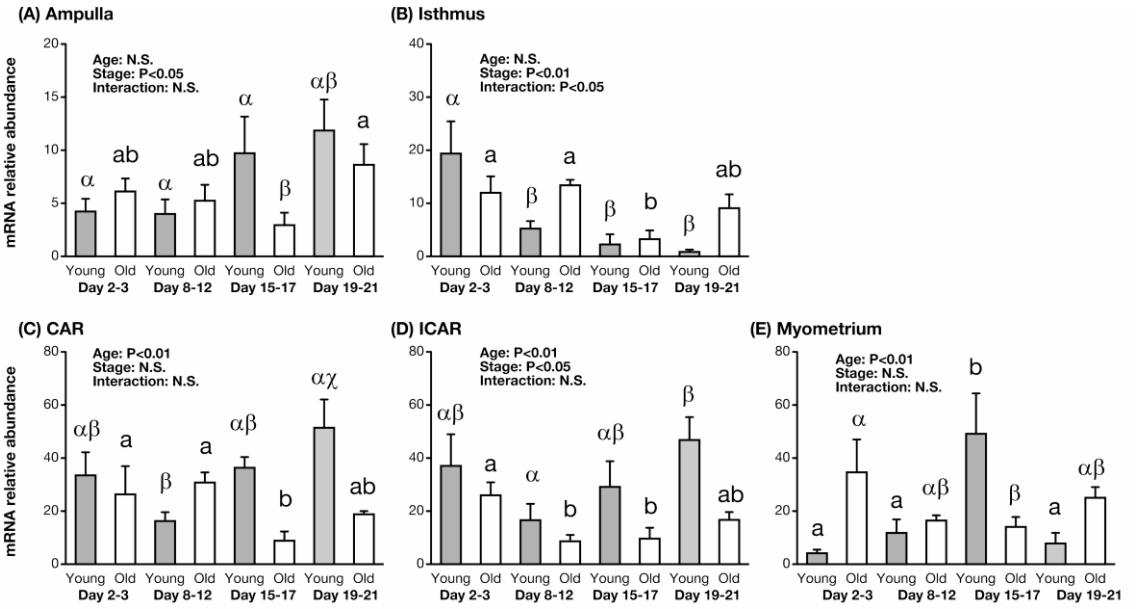

718

719

720 **Fig. 8**. Relative *HSP47* mRNA levels (mean ± SEM) in the ampulla (A), isthmus (B),
721 CAR (C), ICAR (D), or Myo (E) in healthy, post-pubertal growing nulliparous heifers
722 (Young group) and old multiparous cows (Old group), as determined via RT-qPCR. Data
723 were normalised to the geometric means of *C2orf29* and *SUZ12* levels. The header in the
724 upper corner of each graph represents the results of two-factor ANOVA followed by
725 Fisher's PLSD test, including the effect of age (Young or Old) and effect of stage and
726 interaction. Greek letters (α, β, or χ) above the grey left-side bars indicate significant
727 between-stage differences in expression in Young samples; letters (a, b or c) above the
728 white right-side bars indicate significant between-stage differences in expression in Old
729 samples (one-factor ANOVA followed by Fisher's PLSD test).
730 N.S. is abbreviation of non-significant.

731

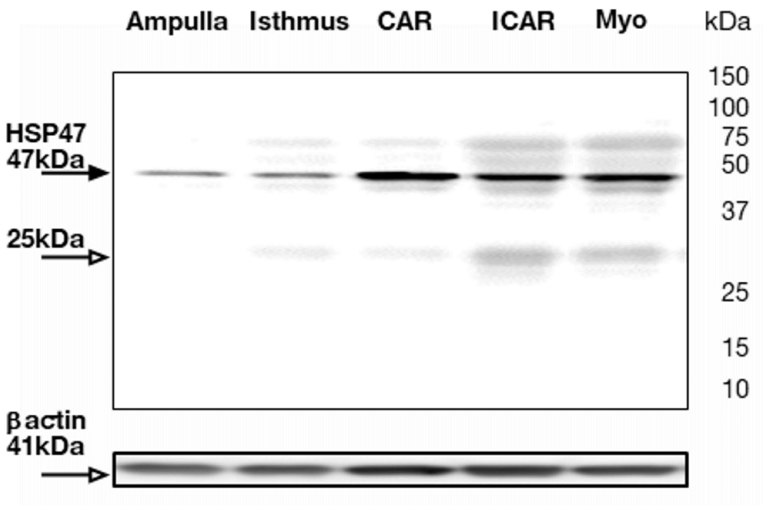

Supplementary Fig. 1. Representative photos of western blotting using another anti-HSP47 mouse monoclonal antibody, clone M16.10A1 (Enzo Life Sciences, Inc., Farmingdale, New York. USA) or anti-βbeta–actin mouse antibodies in extracts from ampulla, isthmus, CAR, ICAR, and myometrium (Myo) in the Young and Old groups.